



Cite this: *Green Chem.*, 2021, **23**, 3392

Received 5th February 2021,
Accepted 1st April 2021

DOI: 10.1039/d1gc00463h

rs.c.li/greenchem

Metal- and additive-free C–H oxygenation of alkylarenes by visible-light photoredox catalysis†

Mustafa Uygur, Jan H. Kuhlmann, María Carmen Pérez-Aguilar, Dariusz G. Piekarski ‡ and Olga García Mancheño ID *

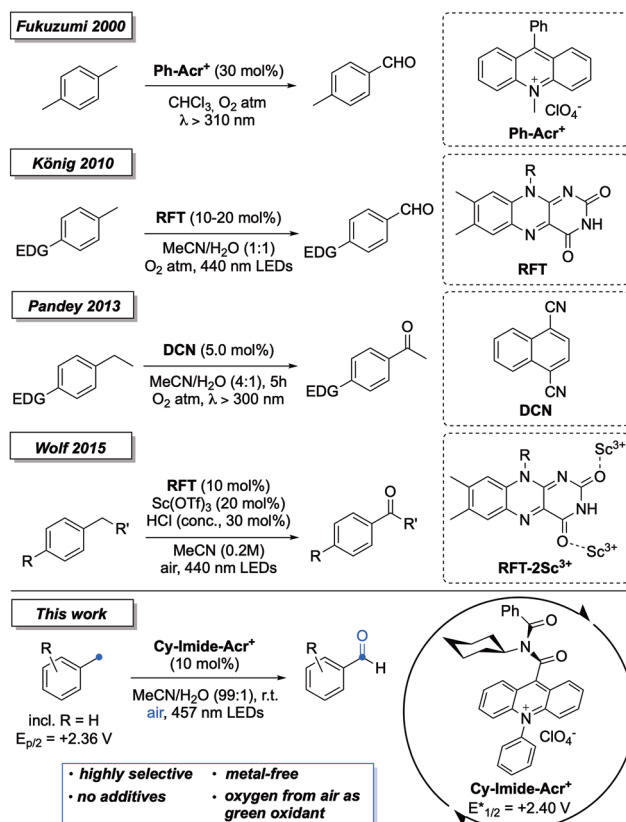
A metal- and additive-free methodology for the highly selective, photocatalyzed C–H oxygenation of alkylarenes under air to the corresponding carbonyls is presented. The process is catalyzed by an imide-acridinium that forms an extremely strong photooxidant upon visible light irradiation, which is able to activate inert alkylarenes such as toluene. Hence, this is an easy to perform, sustainable and environmentally friendly oxidation that provides valuable carbonyls from abundant, readily available compounds.

Introduction

The direct and selective oxygenation of alkylarenes has significant importance in the synthesis of aldehydes and ketones,¹ which are applied as key intermediates in the production of fine chemicals such as agricultural products, dyes and pharmaceutical compounds.² In the last few years, a variety of methodologies have been developed mostly based on transition metal catalysts such as Co, Fe, Pd, Cu or Mn,³ providing the corresponding oxygenation products in good yields. However, the necessity of additives and the requirement of harsh conditions, in particular, elevated temperatures and high oxygen pressure, lead to a lack of sustainability, as well as selectivity.⁴

Visible light photoredox catalysis has recently emerged as a sustainable and powerful alternative,^{5,6} especially with the development of organic dyes as photocatalysts⁷ with highly oxidative excited states (Scheme 1). Already in 2000, Fukuzumi *et al.* reported the light induced photooxidation of xylenes ($E_{p/2} = \sim +2.20$ V vs. SCE)⁸ in the presence of 10-methyl-9-phenylacridinium (Ph-Acr⁺) perchlorate, giving the corresponding methyl-substituted benzaldehydes in good to excellent yields with high selectivity towards the monooxygenation product.^{9,10} Unfortunately, the more challenging substrate toluene ($E_{p/2} = \sim +2.36$ V vs. SCE)⁸ only gave 3% of conversion under the applied conditions.¹¹ Further efforts with 10-methyl-9-mesitylacridinium (Mes-Acr⁺) were again only effective with xylenes or electron-rich substrates,¹² while proving efficient in the

benzylic oxygenation to ketones of activated systems such as diarylmethanes.¹³ In 2010, König and co-workers reported the flavin (RFT) catalyzed C–H oxidation of alkylarenes to the corresponding aldehydes and ketones.¹⁴ The carbonyl compounds were obtained in excellent selectivity, however, the



Scheme 1 C–H oxygenation of alkylarenes by photoredox catalysis.

Organic Chemistry Institute, Westfälische Wilhelms University Münster, Correnstraße 36, 48149 Münster, Germany. E-mail: olga.garcia@uni-muenster.de

† Electronic supplementary information (ESI) available: General procedures and representative analytical data, complete optimization studies, mechanistic experiments and DFT calculations. See DOI: 10.1039/d1gc00463h

‡ Current affiliation: Institute of Physical Chemistry, Polish Academy of Sciences Kasprzaka 44/52, 01-224, Warsaw.

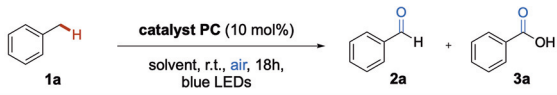
scope was limited to few electron-rich arenes and the catalyst loading had to be increased to 20 mol% in some cases. In 2013, Pandey *et al.* applied 1,4-dicyanonaphthalene (DCN) as a photocatalyst in the C–H oxygenation of alkylarenes, affording the corresponding ketones in moderate to good yields in short reaction times.¹⁵ However, selectivity issues were encountered, leading to mixtures of the alcohol intermediate and the desired ketone. Additionally, the scope of this process was again limited to electron-rich aromatics. Two years later, Wolf *et al.* reported benzylic C–H oxidation in the presence of a flavin–scandium complex.¹⁶ With the additional Lewis acid as an additive, the excited state potential of flavin could be boosted from $E_{1/2}^*$ ($^1\text{RFT}^*/^2\text{RFT}^-$) = +1.67 V to +2.45 V *vs.* SCE. With an excess of concentrated hydrochloric acid, they were able to oxidize toluene and its derivatives in moderate to good yields.

In order to overcome some of the current limitations of reactivity and selectivity in visible light photocatalytic oxidation reactions, we have recently developed a new family of 9-imide-acridinium catalysts capable of forming remarkable strong oxidants in their excited state.¹⁷ Continuing our investigations in this field, we herein present a direct C–H oxygenation methodology implying the powerful photooxidant Cy-Imide-Acr⁺ ($E_{1/2}^*$ = +2.40 V *vs.* SCE)¹⁷ and additive-free, mild conditions to obtain highly selective processes (Scheme 1, bottom).

Results and discussion

We started our investigations with the optimization of the reaction conditions for the visible light photocatalyzed C–H oxygenation of toluene as one of the most challenging compounds in the presence of various acridinium photocatalysts, which form strong oxidants upon visible light irradiation (Table 1). Hereby, commercially available Fukuzumi catalyst **PC I** ($E_{1/2}^*$ = +2.18 V *vs.* SCE)⁷ led to the formation of the desired aldehyde in 15% yield (entry 1), while both acridinium salts **PC II** ($E_{1/2}^*$ ~ +2.10 V *vs.* SCE)^{18a} and **PC IV** ($E_{1/2}^*$ = +1.65 V *vs.* SCE),^{18b} which were previously developed by the Nicewicz group, only gave traces of benzaldehyde in our preliminary studies (entries 2 and 4). While these results can be explained by insufficient excited state potentials of the above-mentioned catalysts to thermodynamically achieve the oxidation of the aromatic system of toluene, a HAT process caused by the decomposition of DCE into chloride anions, which can be subsequently oxidized to Cl-radicals, cannot be excluded. To our delight, imide-acridinium salt **PC III** was able to conduct the oxidation (entry 3). In this case, benzaldehyde **2a** was formed in 36%, while benzoic acid (**3a**) was generated in traces. An extensive solvent screening was then performed (entries 5–7, see also the ESI†). The use of MeCN as a solvent led to a notable improvement of the yield to 51% and a **2a**:**3a** selectivity of 10:1. The concentration effect was also analyzed (entries 8–10). On the one hand, higher concentrations and an increase in the volume of air in the reaction vial led to a loss

Table 1 Optimization of the oxygenation reaction of toluene (**1a**)^a

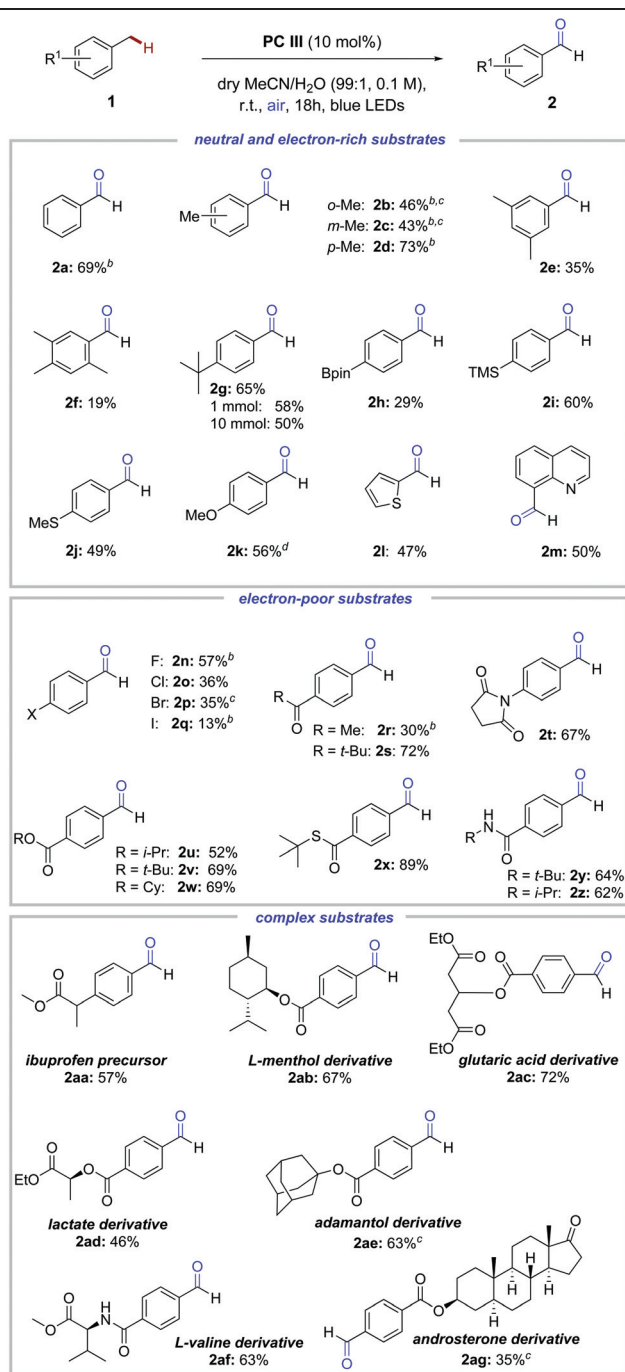


Entry	PC	Dry solvent ([M])	Yield 2a ^b (%)	Yield 3a ^b (%)
1	PC I	DCE (0.1)	15	0
2	PC II	DCE (0.1)	7	0
3	PC III	DCE (0.1)	36	Traces
4	PC IV	DCE (0.1)	1	0
5	PC III	CHCl ₃ (0.1)	33	Traces
6	PC III	TFE (0.1)	2	0
7	PC III	MeCN (0.1)	51	5
8	PC III	MeCN (0.13)	33	6
9	PC III	MeCN (0.2)	31	3
10	PC III	MeCN (0.05)	34	0
11 ^c	PC III	MeCN (0.1)	0	0
12 ^d	PC III	MeCN (0.1)	0	83
13	PC III	dry MeCN/H ₂ O (99 : 1; 0.1)	69	0

^a All reactions were performed on a 0.1 mmol scale using 10 mol% of photocatalyst **PC** in closed vials under an air atmosphere. The vials were irradiated from the bottom plane with blue LEDs (457 nm) for 18h. ^b Yields were determined by GC-FID with *n*-hexadecane as the internal standard. ^c Reaction was degassed and performed under an Ar atmosphere. ^d Reaction performed open to air.

of selectivity due to the competitive formation of benzoic acid (entries 7 and 8). On the other hand, the dilution to 0.05 M resulted in the selective formation of benzaldehyde, however, no significant improvement of the yield of **2a** was monitored (entry 10; 34% of **2a**). In the next step, the importance of oxygen for the reaction outcome was analyzed. No conversion of the starting material was detected when the reaction mixture was degassed and run under an argon atmosphere (entry 11), while the exclusive formation of benzoic acid was observed when the reaction was performed open to air (entry 12; 83% of **3a**). Finally, the impact of the amount of water was explored (see the ESI† for details). Thus, various mixtures of dry MeCN and H₂O as solvents were tested, resulting in the completely selective formation of benzaldehyde in a good yield of 69% when using a 99 : 1 MeCN : H₂O mixture (entry 13).

With the optimized conditions in hand, the scope of our methodology was tested by exploring various methyl-substituted benzenes and heteroaromatic derivatives (Table 2). The reaction with the different regioisomers of xylene led to the corresponding benzaldehydes **2b–d** in good yields and excellent selectivity (monooxygenation and without any overoxidation to the benzoic acids **3**). A similar monooxidation process was observed with mesitylene, resulting in the formation of the desired aldehyde **2e** in 35% yield.¹⁹ Additionally, the use of the bulkier alkylarene durene gave the corresponding aldehyde

Table 2 Scope of aldehyde synthesis from toluene derivatives^a

^aAll reactions were performed on a 0.1 mmol scale. Yields were obtained after flash column chromatography. ^bYields were determined by GC-FID with *n*-hexadecane as the internal standard. ^cReactions were carried out in dry DCE (0.1 M) to enhance the yield or favor the solubility of the substrates. ^dThe reaction was performed with PC IV as the catalyst and 1.0 equiv. of 2,6-lutidine under an O₂ atmosphere.

in a moderate 19% yield, most likely caused by steric reasons, as well as the increasing potential difference between 1,2,4,5-tetramethylbenzene ($E_{p/2} = +1.75$ V vs. SCE)²⁰ and excited state photocatalyst PC III. Further substituents at the *para*-position

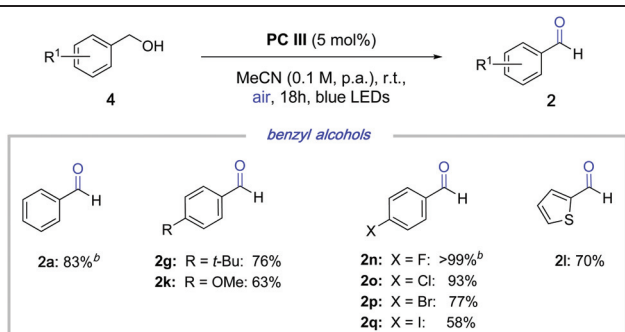
such as a *tert*-butyl group and oxidation labile functional groups such as boron, silicon and thioether moieties gave the desired aldehyde products **2g–j** in moderate to good yields (29–65%). Hence, in the case of the pinacol boronate **1h**, the hydroxylation product to the corresponding phenol was not observed under the employed oxidative photoredox conditions.²¹ Additionally, the oxygenation reaction of the substrate **1g** could be scaled up 100 fold, giving the desired product **2g** in a good yield of 50% with again excellent chemoselectivity. Interestingly, substrate **1k** could only be transformed into the desired aldehyde **2k**, when PC IV was applied as catalyst with 1.0 equivalent of 2,6-lutidine as additive under an oxygen atmosphere, while the use of imide-acridinium salt PC III under the exactly same reaction conditions did not result in any conversion of **1k**. We assume that this observation is caused by the similarity between the redox potential of excited catalyst PC IV ($E_{1/2}^* = +1.65$ V vs. SCE)^{18b} and the potential that is required to oxidize the aromatic system of **1k** ($E_{p/2} = +1.52$ V vs. SCE),²² while the large gap between the excited-state potential PC III and the substrate leads to an inefficient electron transfer process. Furthermore, our investigations demonstrated that the presence of an additional base is essential for the successful oxygenation of **1k**, which is necessary for the deprotonation step once the aromatic system is oxidized. In the case of neutral and electron-poor substrates, this step takes place spontaneously after the single electron oxidation occurs. Switching the substrate class to heteroarenes such as 2-methyl-thiophene (**1l**) and 8-methylquinoline (**1m**) showed that these compounds were well-suitable for the standard method with PC III as the photocatalyst and gave the related aldehydes in 47–50% yield. Next, we turned our focus on arenes containing electron withdrawing groups. Thus, halides were well tolerated, giving chemoselectively the corresponding aldehydes **2n–p** in good yields (35–57%), except for 4-iodotoluene (**1q**) that led to the formation of aldehyde **2q** in only 13% yield. This result can be reasoned by a more favorable oxidation on the iodine atom as a competitive side-reaction or by the high potential difference between PC III* and **1q**. Further electron withdrawing functionalities at the *para* position, such as acetyl moieties (**2r** and **2s**) and an imide group (**2t**), gave the desired products in moderate to good yields (30–72%). Moreover, esters (**1u–1w**), a thioester (**1x**) and amide functionalities (**1y** and **1z**) were extremely well tolerated under the optimized reaction conditions, leading to the explicit formation of the corresponding aldehydes in good to excellent yields (52–89%). Finally, to prove the applicability of our methodology, we decided to perform the C–H oxygenation of more complex structures. Thus, the oxygenation of methyl protected ibuprofen **1aa** led to the formation of aldehyde **2aa** (57%) after the C–C bond cleavage at the benzylic position. Furthermore, our process was extremely compatible with derivatives of L-menthol, glutaric acid, lactate, adamantol, L-valine and androsterone, giving the desired aldehydes **2ab** to **2ag** in good isolated yields (35–72%) and excellent chemoselectivity.

Next, we wondered if our catalytic system would also be effective for the selective oxidation of benzylic alcohols to the

corresponding aldehydes. A small screening of the reaction conditions with benzyl alcohol (**4a**) as the substrate demonstrated the exclusive formation of benzaldehyde (**2a**) in a good yield of 83%. Additionally, the catalyst loading could be decreased to 5 mol%, indicating that the oxidation of benzylic alcohols is less challenging than those of the toluene derivatives. The compatibility of our system with various functionalities was tested in the next step, resulting in the formation of the desired aldehydes again in excellent selectivity in all cases (Table 3). Hereby, neutral as well as electron donating groups such as *tert*-butyl and methoxy groups at the *para* position gave the desired products **2g** and **2k** in good yields (63–76%). Moreover, different halides gave the corresponding aldehydes **2n** to **2q** in good to excellent yields (58% to >99%), while the heterocyclic substrate **4l** could be transformed into the desired product successfully (**2l**, 70%).

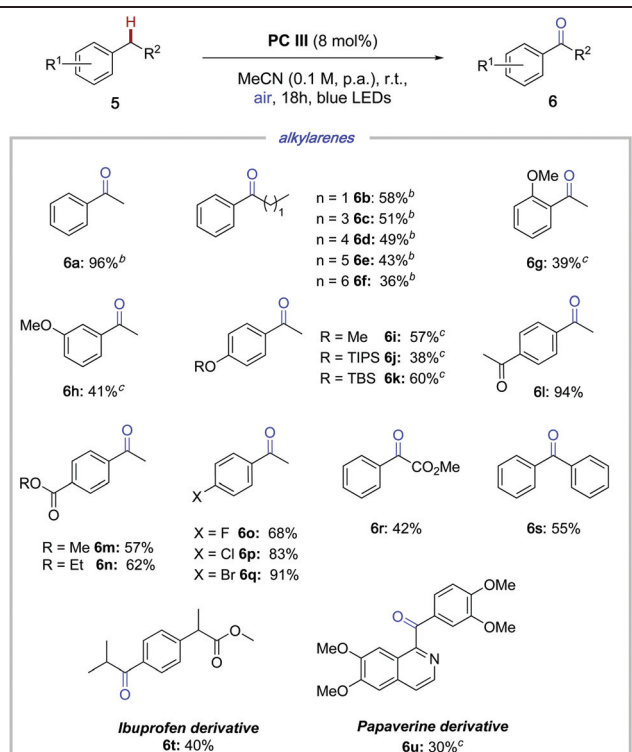
With these results in hand, we focused our attention on the synthesis of ketones (Table 4). Initially, we started our investigations with ethylbenzene **5a** ($E_{\text{ox}} = +2.14$ V vs. SCE).¹⁶ After screening of various reaction conditions (see the ESI†), we could identify the optimal reaction conditions to be the use of 8 mol% of **PC III** in p.a. MeCN (0.1 M) as a solvent in a closed vial under an air atmosphere. Accordingly, the desired ketone **6a** was obtained in an excellent yield of 96%. Next, the impact of the length of the alkyl chain connected to the aromatic system was analyzed. In all cases, the desired ketones **6b–f** were obtained in moderate to good yields (36% to 58%), while a decrease of the yield with an increase in the chain length was observed. The functional group tolerance was then investigated by variations in the substitution pattern in the aromatic system. As in the case of toluene derivatives, the oxygenation of various methoxy substituted ethyl benzenes (**5g–5i**) and different silyl protected substrates (**5j** and **5k**) was only successful in the presence of catalyst **PC IV** and 1.0 equivalent of 2,6-lutidine, leading to the formation of the desired products in moderate to good yields (39–60%). Contrarily, electron withdrawing groups such as a ketones, esters and halides (**5l–5q**) gave the corresponding ketones in good to excellent yields (57–94%) in the presence of imide-acridinium salt **PC III**.

Table 3 Scope of aldehyde synthesis from benzylic alcohols^a



^aAll reactions were performed on a 0.1 mmol scale. Yields were obtained after flash column chromatography. ^bYields were determined by GC-FID with *n*-hexadecane as the internal standard.

Table 4 Scope of ketone synthesis^a

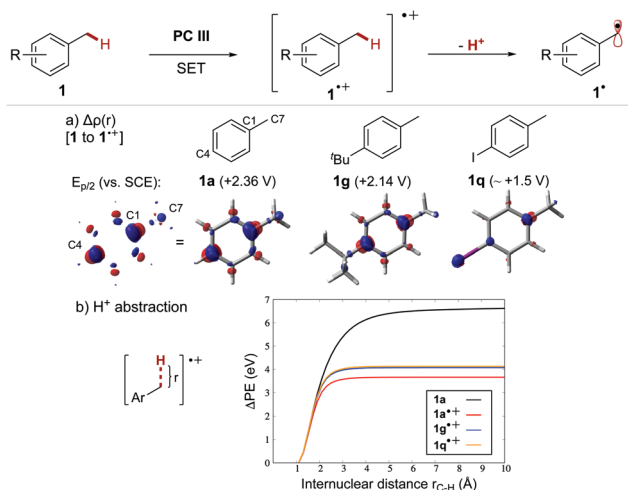


^aAll reactions were performed on a 0.1 mmol scale. Yields were obtained after flash column chromatography. ^bYields were determined by GC-FID with *n*-hexadecane as the internal standard. ^cThe reaction was performed with **PC IV** as the catalyst and 1.0 equiv. of 2,6-lutidine under an O₂ atmosphere.

Furthermore, acetophenones bearing substituents at the alkyl chain were also well tolerated, allowing the introduction of ester and aryl groups (**6r–s**, 42–55%). Once again, the methodology was applied on more complex structures such as ibuprofen **5t** and papaverine **5u** derivatives, resulting in the formation of the desired ketones (30–40%) in excellent selectivity.

Motivated by these results, we decided to explore the mechanism of the photocatalyzed C–H oxygenation reaction. We started our investigations by fluorescence quenching experiments of imide-acridinium photocatalyst **PC III** in the presence of various amounts of toluene **1a** (see the ESI† for details). As already indicated by the electrochemical data, efficient quenching of the excited state photocatalyst ($E_{1/2}^* = +2.40$ V vs. SCE)¹⁷ by toluene ($E_{p/2} = +2.36$ V vs. SCE)⁸ was observed ($K_{\text{SV}} \sim 66.1$ M⁻¹), illustrating that the oxygenation reaction is initiated by the direct interaction of both species **PC III*** and **1a**.

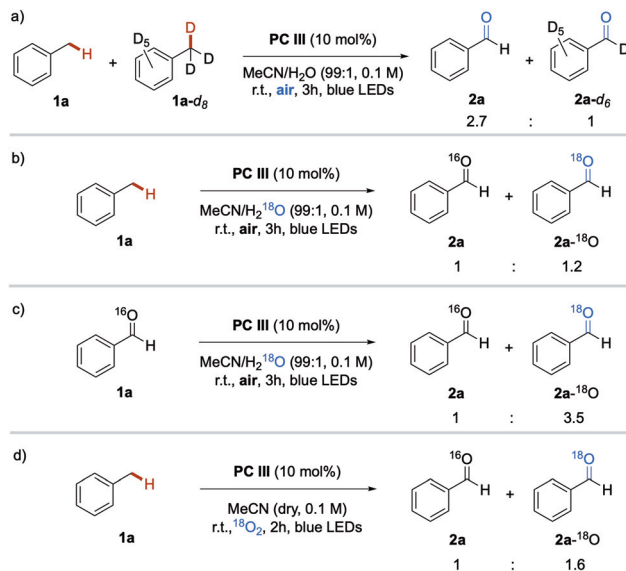
Furthermore, DFT-based calculations on the initial steps to form the postulated reactive key benzylic radical intermediate **1*** from methylbenzenes were carried out using the Gaussian16 program²³ (Scheme 2, see the ESI† for details). The structures were optimized in the gas phase at the DFT-b3lyp-GD3BJ/def2tzvp level of theory accounting for Grimme's dispersion with Becke–Johnson damping correction (GD3BJ).²⁴



Scheme 2 Mechanistic investigations on the first SET oxidation step and the subsequent deprotonation: (a) electron density difference $\Delta\rho(r)$ between **1a** and its radical cation **1a^{•+}** (at isovalues of $\pm 0.008 \text{ e}^- \text{ au}^{-3}$). (b) Rigid scan along the benzylic C-H bond for the deprotonation step from **1^{•+}** calculated at the DFT-b3lyp-GD3BJ/def2tzvp level of theory.

Initially, we examined the generation of the radical cation **1^{•+}**. Thus, the calculated electron density difference ($\Delta\rho(r)$) between the neutral substrate **1** and its oxidized radical cation **1^{•+}** in Franck-Condon type transition provides the accumulation and depletion of the electron density, which are shown in red and blue, respectively (Scheme 2a). For this purpose, three representative methylbenzene substrates **1a**,⁸ **1g**²⁵ and **1q**²⁶ with distinct oxidation potentials were chosen. A decrease of electron density in closer proximity to the benzylic H-atom was found in all cases, while for **1q** a more remarkable reduction of electron density was observed at the easily oxidizable iodine atom. Moreover, it is clearly seen that the single electron transfer (SET) occurs mainly from the aromatic ring (C1 and C4 positions) but also, especially for toluene (**1a**), from the C7 of the methyl group. Hence, once the first SET to form the radical cation intermediate takes place, H abstraction *via* benzylic C-H bond cleavage is facilitated.²⁷ The second step was next studied, for which a rigid potential energy (PE) curve scan along the C-H bond was performed considering that the H-abstraction occurs without relaxation of the system after the ionization (Scheme 2b). The C-H bond cleavage involves a significantly less dissociation energy ($\Delta E \sim 3 \text{ eV}$) for the radical cation **1a^{•+}** than for the neutral toluene molecule (6.68 *vs.* 3.75 eV for **1a** and **1a^{•+}**, respectively). Moreover, the required energy to dissociate the C-H bond varies as a function of the substituent, *i.e.*, it increases in the order: **1a^{•+}** (3.75 eV) < **1q** (4.12 eV) \cong **1g** (4.15 eV).

Subsequently, we decided to study the kinetic isotope effects (KIE) in this reaction to evaluate if the benzylic proton cleavage is rate determining. Therefore, the standard reaction was performed in the presence of a mixture of toluene-*h*₈ (**1a**) and toluene-*d*₈ (**1a-d**₈) (Scheme 3a). The analysis of the reaction mixture by GC-MS after three hours gave the exclusive formation of benzaldehyde-*h*₆ (**2a**) and benzaldehyde-*d*₆ (**2a-d**₆)



Scheme 3 Mechanistic investigations on the oxygenation reaction. (a) Competitive KIE study. (b) Standard reaction in the presence of labeled water. (c) Control experiment. (d) Standard reaction in the presence of labeled oxygen.

with a KIE of 2.7. This primary isotope effect suggests the proton abstraction step from toluene **1a^{•+}** to the benzylic radical **1a[•]** as the rate-determining step. Additionally, the standard reaction was performed in the presence of ¹⁸O labeled water in order to find out the oxygen source (Scheme 3b). The analysis of the crude mixture by GC-MS showed a 1:1.2 ratio of benzaldehyde-¹⁶O (**2a**) to benzaldehyde-¹⁸O (**2a-¹⁸O**) after three hours of reaction time. In order to evaluate the possible oxygen-isotope exchange on the formed benzaldehyde under the photocatalytic conditions, a control experiment was conducted by replacing toluene with benzaldehyde-¹⁶O (Scheme 3c). The analysis of the reaction mixture disclosed a 1:3.5 ratio of **2a** to **2a-¹⁸O**, indicating a very fast exchange of oxygen, once benzaldehyde is formed. Finally, the model reaction was performed in the presence of an ¹⁸O₂ atmosphere, giving the desired products **2a** and **2a-¹⁸O** in a ratio of 1:1.6 (Scheme 3d). Taking these experiments into account, we concluded that for the oxygenation process, the main source of oxygen comes from the air and not from water, and the isotope exchange observed occurs by reversible addition of water to the carbonyl group. Moreover, in order to detect the generated radical species in the reaction mixture, the standard reaction was performed in the presence of 1.2 equivalents of 2,2,6,6-tetramethylpiperidinyloxy (TEMPO) as a radical trap. Hereby, the TEMPO-benzylic radical adduct **7** could be detected by HRMS, while the homocoupling product **8** could be identified by GC-MS measurements. In order to identify further oxygen-centered radical intermediates, various EPR measurements were conducted, however, none of the desired intermediates could be detected. Nevertheless, a reaction monitored by ¹H-NMR proved the presence of hydroperoxide intermediate **11** as well as benzylic alcohol **4a** in the reaction

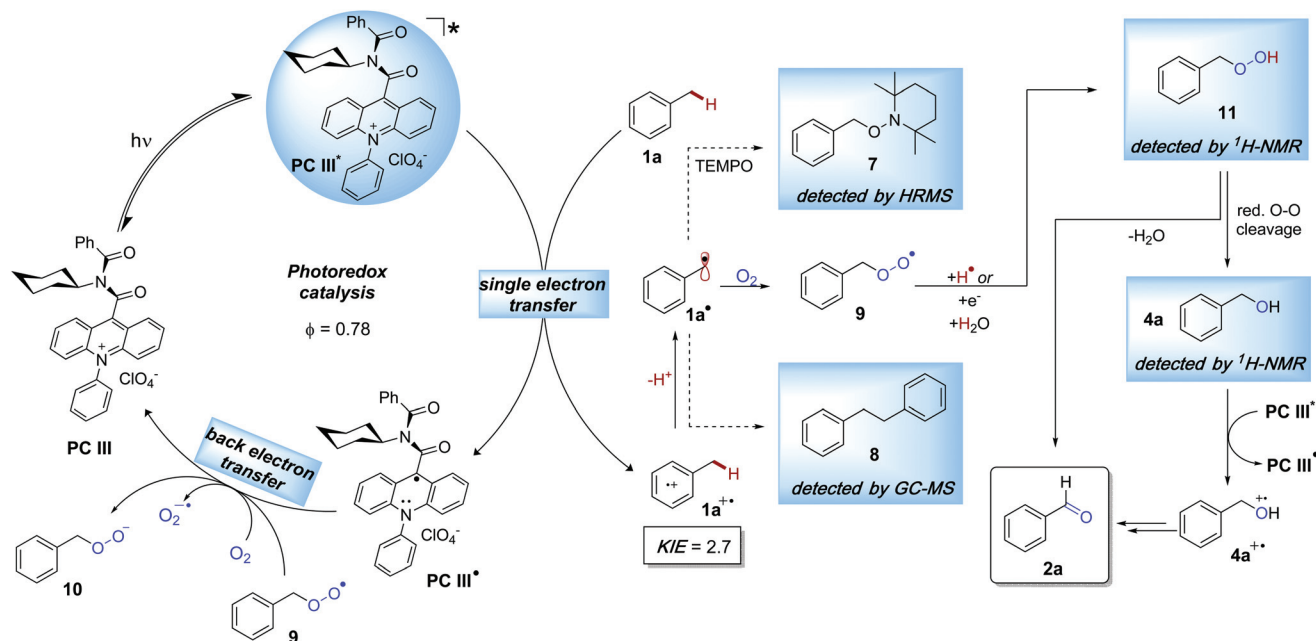


Fig. 1 Proposed reaction mechanism for photocatalytic C–H oxidation.

mixture (see the ESI† for details). Finally, the reaction quantum yield was determined by standard ferrioxalate actinometry to figure out if a radical chain process is involved.²⁸ Hereby, a fluorescence quantum yield of $\phi = 0.78$ was obtained, suggesting that a radical chain process is not the predominant pathway ($\phi \leq 1$).

Based on the previous reports⁹ and taking all the previous observations into account, the following plausible reaction mechanism can be proposed (Fig. 1): Imide-acridinium photocatalyst **PC III** reaches its excited state upon irradiation by visible light, leading to the formation of an extremely strong photooxidant **PC III***. This species is able to undergo a single electron oxidation step with toluene (**1a**), giving rise to radical cationic intermediate **1a^{•+}** and reduced photocatalyst **PC III•**, which reaches its ground state by back electron transfer (BET) either to oxygen from the air or to peroxy-intermediate **9**, which gives rise to **10**. Next, benzylic radical **1a•** is generated after proton abstraction of **1a^{•+}**, which is subsequently trapped by oxygen, leading to peroxy-species **9**, which leads to benzyl hydroperoxide **11** either after H-radical abstraction or after BET and protonation of **10**. Consequently, intermediate **11** can lead to the formation of benzaldehyde **2a** by elimination of water and benzylic alcohol **4a** by reductive cleavage of the O–O bond. In the final step, the alcohol **4a** is oxidized to the corresponding aldehyde **2a** by excited state photocatalyst **PC III***.

Conclusions

In conclusion, we were able to develop a metal- and additive-free process for the visible light photocatalyzed C–H oxygenation of toluene and its derivatives. The desired aldehydes were obtained

in good yields with excellent chemoselectivity, while the carboxylic acid formation could be fully suppressed. Furthermore, selective generation of carboxylic acids could be observed when the reactions were performed in open air. Additionally, this methodology could be further expanded to benzyl alcohols and alkylarenes, which gave the corresponding aldehydes and ketones in excellent yields. Due to the extremely mild reaction conditions, various functional groups were well-tolerated in both aldehyde and ketone generation processes. Additionally, our methodology was compatible with various complex structures, such as natural compounds or drug derivatives. Mechanistic investigations suggested that the oxygenation reaction is induced by the direct interaction between the excited state photocatalyst and the substrate molecules, while a radical chain process could be excluded as the predominant pathway by quantum yield measurements. The analysis of the kinetic isotope effect illustrated that the abstraction of a proton from the oxidized alkylbenzene substrate, which leads to the formation of the benzylic key radical intermediate, is involved in the rate-determining step. Furthermore, experiments with labeled water and oxygen demonstrated that the main oxygen source is the molecular oxygen from the air and not the co-solvent water.

Conflicts of interest

There are no conflicts to declare.

Acknowledgements

The Deutsche Forschungsgemeinschaft (DFG) is gratefully acknowledged for generous support.

Notes and references

- (a) N. Jiao and S. S. Stahl, *Green Oxidation in Organic Synthesis*, Wiley, Hoboken, NJ, 2019; (b) J.-E. Bäckvall, *Modern Oxidation Methods*, Wiley, 2nd edn, 2011; (c) K. Chen, P. Zhang, Y. Wanga and H. Li, *Green Chem.*, 2014, **16**, 2344.
- (a) S. Warren, *Chemistry of the Carbonyl Group - Programmed Approach to Organic Reaction Method*, Wiley, London, New York, 1974; (b) O. Junzo, *Modern Carbonyl Chemistry*, Wiley, Weinheim, 2000. See e.g. also: (c) B. E. Kahn and R. D. Rieke, *Chem. Rev.*, 1988, **88**, 733; (d) K. A. Jørgensen, *Angew. Chem., Int. Ed.*, 2000, **39**, 3558; (e) L. Ravindar, R. Lekkala, K. P. Rakesh, A. M. Asiri, H. M. Marwanib and H.-L. Qin, *Org. Chem. Front.*, 2018, **5**, 1381.
- Selected examples: (a) Y.-F. Wang, H. Chen, X. Zhu and S. Chiba, *J. Am. Chem. Soc.*, 2012, **134**, 11980; (b) P. Y. Choy and F. Y. Kwong, *Org. Lett.*, 2013, **15**, 270; (c) V. S. Thirunavukkarasu, S. I. Kozhushkov and L. Ackermann, *Chem. Commun.*, 2014, **50**, 29; (d) A. C. Lindhorst, S. Haslinger and F. E. Kühn, *Chem. Commun.*, 2015, **51**, 17193; (e) Y.-F. Liang and N. Jiao, *Acc. Chem. Res.*, 2017, **50**, 1640; (f) N. Saueremann, T. H. Meyer, C. Tian and L. Ackermann, *J. Am. Chem. Soc.*, 2017, **139**, 18452; (g) F. Burg, M. Gicquel, S. Breitenlechner, A. Pöthig and T. Bach, *Angew. Chem., Int. Ed.*, 2018, **57**, 2953; (h) S. Fukuzumi, Y.-M. Lee and W. Nam, *ChemSusChem*, 2019, **12**, 3931.
- See e.g.: (a) C. Yuan, Y. Liang, T. Hernandez, A. Berriochoa, K. N. Houk and D. Siegel, *Nature*, 2013, **499**, 192; (b) J. Börgel, L. Tanwar, F. Berger and T. Ritter, *J. Am. Chem. Soc.*, 2018, **140**, 16026.
- Selected reviews: (a) T. P. Yoon, M. A. Ischay and J. Du, *Nat. Chem.*, 2010, **2**, 527; (b) J. M. R. Narayanam and C. R. J. Stephenson, *Chem. Soc. Rev.*, 2011, **40**, 102; (c) J. Xuan and W.-J. Xiao, *Angew. Chem., Int. Ed.*, 2012, **51**, 6828; (d) Y. Xi, H. Yi and A. Lei, *Org. Biomol. Chem.*, 2013, **11**, 2387; (e) C. K. Prier, D. A. Rankic and D. W. C. MacMillan, *Chem. Rev.*, 2013, **113**, 5322; (f) M. Reckenthäler and A. G. Griesbeck, *Adv. Synth. Catal.*, 2013, **355**, 2727; (g) M. N. Hopkinson, B. Sahoo, J. L. Li and F. Glorius, *Chem. – Eur. J.*, 2014, **20**, 3874; (h) D. M. Schultz and T. P. Yoon, *Science*, 2014, **343**, 985; (i) J. Twilton, C. Le, P. Zhang, M. H. Shaw, R. W. Evans and D. W. C. MacMillan, *Nat. Rev. Chem.*, 2017, **1**, 0052; (j) M. Silvi and P. Melchiorre, *Nature*, 2018, **554**, 41; (k) Y. Q. Zou, F. M. Hörmann and T. Bach, *Chem. Soc. Rev.*, 2018, **47**, 278. Selected examples for heterogeneous photocatalytic oxygenation reactions: (l) K. Tamai, K. Murakami, S. Hosokawa, H. Asakura, K. Teramura and T. Tanaka, *J. Phys. Chem. C*, 2017, **121**, 22854; (m) P. Chen, Y. Li, C. Xiao, L. Chen, J.-K. Guo, S. Shen, C.-T. Au and S.-F. Yin, *ACS Sustainable Chem. Eng.*, 2019, **7**, 17500; (n) C. M. Cova, A. Zuliani, M. J. Muñoz-Batista and R. Luque, *ACS Sustainable Chem. Eng.*, 2019, **7**, 1300; (o) K. Su, H. Liu, B. Zeng, Z. Zhang, N. Luo, Z. Huang, Z. Gao and F. Wang, *ACS Catal.*, 2020, **10**, 1324; (p) F. Liu, C.-X. Xiao, L.-H. Meng, L. Chen, Q. Zhang, J.-B. Liu, S. Shen, J.-K. Guo, C.-T. Au and S.-F. Yin, *ACS Sustainable Chem. Eng.*, 2020, **8**, 1302.
- Selected reviews on photocatalyzed C–H functionalization: (a) L. Shi and W. Xia, *Chem. Soc. Rev.*, 2012, **41**, 7687; (b) J. Xie, H. Jin and C. Zhu, *Tetrahedron Lett.*, 2014, **55**, 36; (c) L. Revathi, L. Ravindar, W.-Y. Fang, K. P. Rakesh and H.-L. Qin, *Adv. Synth. Catal.*, 2018, **360**, 4652; (d) X. Zhang, K. P. Rakesh, L. Ravindar and H.-L. Qin, *Green Chem.*, 2018, **20**, 4790; (e) M. Uygur and O. García Mancheño, *Org. Biomol. Chem.*, 2019, **17**, 5475; (f) L. Guillemard and J. Wencel-Delord, *Beilstein J. Org. Chem.*, 2020, **16**, 1754.
- N. A. Romero and D. A. Nicewicz, *Chem. Rev.*, 2016, **116**, 10075.
- H. Roth, N. Romero and D. Nicewicz, *Synlett*, 2016, 714.
- (a) K. Ohkubo and S. Fukuzumi, *Org. Lett.*, 2000, **2**, 3647; (b) K. Ohkubo, K. Suga, K. Morikawa and S. Fukuzumi, *J. Am. Chem. Soc.*, 2003, **125**, 12850.
- Selected recent reviews and reports on photocatalyzed C–H oxygenations: (a) C. Bian, A. K. Singh, L. Niu, H. Yi and A. Lei, *Asian J. Org. Chem.*, 2017, **6**, 386; (b) Y. Zhang, W. Schilling and S. Das, *ChemSusChem*, 2019, **12**, 2898; (c) B. Mühlendorf, U. Lennert and R. Wolf, Coupling photo-redox and biomimetic catalysis for the visible-light-driven oxygenation of organic compounds, in *Chemical Photocatalysis*, ed. B. König, De Gruyter, 2nd edn, 2020, ch. 10. See also: (d) K. Suga, K. Ohkubo and S. Fukuzumi, *J. Phys. Chem. A*, 2005, **109**, 10168; (e) K. Ohkubo, K. Suga and S. Fukuzumi, *Chem. Commun.*, 2006, 2018; (f) H. J. Xu, X. L. Xu, Y. Fu and Y. S. Feng, *Chin. Chem. Lett.*, 2007, **18**, 1471; (g) N. Tada, K. Hattori, T. Nobuta, T. Miura and A. Itoh, *Green Chem.*, 2011, **13**, 1669; (h) S. Fukuzumi, K. Doi, A. Itoh, T. Suenobu, K. Ohkubo, Y. Yamada and K. D. Karlin, *Proc. Natl. Acad. Sci. U. S. A.*, 2012, **109**, 15572; (i) K. Ohkubo, K. Mizushima and S. Fukuzumi, *Res. Chem. Intermed.*, 2013, **39**, 205; (j) P. Dongare, I. MacKenzie, D. Wang, D. A. Nicewicz and T. J. Meyer, *Proc. Natl. Acad. Sci. U. S. A.*, 2017, **114**, 9279; (k) M. Lesieur, C. Genicot and P. Pasau, *Org. Lett.*, 2018, **20**, 1987.
- Preliminary report with the photounstable AcrH⁺: M. Fujita and S. Fukuzumi, *J. Mol. Catal.*, 1994, **90**, L225.
- K. Ohkubo, K. Mizushima, R. Iwata, K. Souma, N. Suzuki and S. Fukuzumi, *Chem. Commun.*, 2010, **46**, 601.
- H. Yi, C. Bian, X. Hu, L. Niu and A. Lei, *Chem. Commun.*, 2015, **51**, 14046.
- R. Lechner, S. Kümmel and B. König, *Photochem. Photobiol. Sci.*, 2010, **9**, 1367.
- G. Pandey, S. Pal and R. Laha, *Angew. Chem., Int. Ed.*, 2013, **52**, 5146.
- (a) B. Mühlendorf and R. Wolf, *Chem. Commun.*, 2015, **51**, 8425. For an alternative RFT-Fe catalytic system, see: (b) B. Mühlendorf and R. Wolf, *Angew. Chem., Int. Ed.*, 2016, **55**, 427.
- (a) A. Gini, M. Uygur, T. Rigotti, J. Alemán and O. García Mancheño, *Chem. – Eur. J.*, 2018, **24**, 12509; (b) A. Gini,

- T. Rigotti, R. Pérez-Ruiz, M. Uygur, R. Mas-Ballesté, I. Corral, L. Martínez-Fernández, V. A. de la Peña O'Shea, O. García Mancheño and J. Alemán, *ChemPhotoChem*, 2019, **3**, 609.
- 18 (a) A. Joshi-Pangu, F. Lévesque, H. G. Roth, S. F. Oliver, L.-C. Champeau, D. A. Nicewicz and D. A. DiRocco, *J. Org. Chem.*, 2016, **81**, 7244; (b) A. R. White, L. Wang and D. A. Nicewicz, *Synlett*, 2019, 827.
- 19 Generally, complete conversion of **1** to the corresponding benzoic acids **3** was observed by performing the reaction open to air, which suggests partial decomposition or polymerization of the formed aldehydes.
- 20 P. Luo, J. P. Dinnocenzo, P. B. Merkel, R. H. Young and S. Farid, *J. Org. Chem.*, 2012, **77**, 1632.
- 21 Pioneer visible light photocatalytic work: (a) Y.-Q. Zou, J.-R. Chen, X.-P. Liu, L.-Q. Lu, R. L. Davis, K. A. Jørgensen and W.-J. Xiao, *Angew. Chem., Int. Ed.*, 2012, **51**, 784. For a recent chemoselective stoichiometric oxidation, see: (b) J. J. Molloy, T. A. Clohessy, C. Irving, N. A. Anderson, G. C. Lloyd-Jones and A. J. B. Watson, *Chem. Sci.*, 2017, **8**, 1551.
- 22 Y. Ashikrai, T. Nokami and J. Yoshida, *J. Am. Chem. Soc.*, 2011, **133**, 11840.
- 23 M. J. Frisch, *et al.*, *Gaussian16 Revision B.01*, Gaussian Inc., Wallingford CT, 2016.
- 24 (a) A. D. Becke, *J. Chem. Phys.*, 1993, **98**, 5648; (b) F. Weigend and R. Ahlrichs, *Phys. Chem. Chem. Phys.*, 2005, **7**, 3297; (c) S. Grimme, S. Ehrlich and L. Goerigk, *J. Comput. Chem.*, 2011, **32**, 1456.
- 25 T. Tajima and T. Fuchigami, *Chem. – Eur. J.*, 2005, **11**, 6192.
- 26 (a) S. Hara, T. Hatakeyama, S.-Q. Chen, K. Ishii, M. Yoshida, M. Sawaguchi, T. Fukuhara and N. Yoneda, *J. Fluorine Chem.*, 1998, **87**, 189; (b) M. Elsherbini and T. Wirth, *Chem. – Eur. J.*, 2018, **24**, 13399; (c) S. Doobary, A. T. Sedikides, H. P. Caldora, D. L. Poole and A. J. J. Lennox, *Angew. Chem., Int. Ed.*, 2020, **59**, 1155; (d) Estimated $E_{p/2}$ using $E_{p/2}(SSCE) = +0.045$ V vs. SCE.
- 27 This is in concordance with the reported increase in acidity of the benzylic protons upon formation of the radical cation with respect to the neutral molecule. See *e.g.*: D. R. Arnold, X. Du and K. M. Henseleit, *Can. J. Chem.*, 1991, **69**, 839.
- 28 M. A. Cismesia and T. P. Yoon, *Chem. Sci.*, 2015, **6**, 5426.